Diffractive Spectroelectrochemistry. Use of Diffracted Light for Monitoring Electrogenerated Chromophores

Paula Rossi, C. William McCurdy, and Richard L. McCreery*

Contribution from the Department of Chemistry, The Ohio State University, Columbus, Ohio 43210. *Received October 28, 1980*

Abstract: When a laser beam strikes an electrode, some of the beam is diffracted away from the main beam into the electrode shadow. If the electrode is oriented such that part of the beam travels parallel to the active surface before diffraction occurs, the diffracted light will be affected strongly by the presence of chromophores near the electrode surface. Absorbance measurements made by using the diffracted light provide a sensitive and fast probe of the generation and decay of electrogenerated chromophores, permitting greatly improved performance compared to previously used spectroelectrochemical techniques. In addition, the diffracted light contains spatial information about the distribution of chromophores within the diffusion layer. Theory and experimental verification for the new method are presented, and the advantages of high sensitivity, fast response, and spatial resolution are discussed.

Electrochemistry has long been employed for the generation and monitoring of reactive species in solution, usually on a time scale of a few seconds down to the submillisecond range. The most common approach involves controlled potential experiments such as voltammetry and chronoamperometry, where the current is monitored and used to deduce mechanistic and thermodynamic information. While methods based on measurement of current have been very widely used with significant success, they often suffer from an inherent lack of selectivity. Controlled potential methods are excellent for generating reactive species, but the observed current may reflect the reactions of several solution species. Particularly with complex reactons of electrogenerated species, the observation of current is often insufficient to deduce a mechanism, or even to measure overall rate constants.

The addition of an optical probe to an electrochemical experiment provides a powerful basis for increased selectivity. Several types of spectroelectrochemical methods have been developed, involving a variety of spectroscopic and electrochemical techniques. The methods involving a combination of UV-vis spectrophotometry and controlled potential methods have been reviewed and their merits and problems discussed.[1-5] A variety of configurations has been used for absorption spectroelectrochemistry, including a beam passing through an optically transparent electrode,[1] a beam reflected off an electrode,[6] internal reflection at the electrode surface,[4] and a beam passing parallel to a planar electrode.[5] These techniques have been used successfully for a variety of problems and have greatly increased the utility of spectroelectrochemistry for studying fast reactions. However, there are some limitations when the techniques are applied to systems with short-lived or weakly absorbing electrogenerated species. The inherent heterogeneous nature of electrochemical processes dictates that all events of interest occur within a thin layer of solution near an electrode surface (thickness $\sim(Dt)^{1/2}$ or ~ 100 μm at 10 s). The thinness of this layer places severe constraints on the optical methods employed to monitor electrogenerated components. For a beam passing through a transparent electrode, the effective path length is very short (~ 100 μm or less) so the technique is insensitive and limited to strong absorbers with relatively long lifetimes. While internal reflection spectroscopy allows one to monitor events very close to the electrode surface, the length of the evanescent wave (~ 1000 Å) dictates a short effective path length.

Several reports from this laboratory have discussed methods to improve the sensitivity of spectroelectrochemical methods by increasing the effective optical path length. A beam reflected off an electrode at glancing incidence allows an improvement in sensitivity by a factor of 100-200 over transparent electrode techniques,[6,7] but higher values were not attainable reliably. A different approach with light passing parallel to the electrode had comparable sensitivity, but was not useful for species with lifetimes less than about 100 ms.[6] In addition, a significant error in the parallel geometry results from diffraction caused by the electrode. This diffraction causes a moderate decrease in sensitivity and limits how close to the electrode one can monitor chromophores. When a reactive species is generated at the electrode, it will not diffuse away very far (e.g., 10 μm for a 100-ms lifetime), so poor performance at short distances represents a serious drawback when monitoring short-lived species. The present effort is directed toward development of a method providing high sensitivity at short times.

Consider a beam of light impinging on an electrode with part of the beam striking the electrode and part of it traveling parallel to the active surface, as shown in Figure 1. Diffraction by the electrode will scatter light away from the main beam, and some diffracted intensity will appear both in the shadow of the electrode and in the region below the beam in Figure 1. This diffraction process will be considered in detail below, but it is important to note that the major contribution to diffracted intensity comes from light passing close to the electrode surface. Clearly light passing distant from the electrode will not be appreciably scattered, so to a first approximation, it is true that the diffracted light has passed through the region of interest close to the electrode. If diffracted intensity were monitored during generation of a chromophore, it should be very sensitive to chromophore concentration. The advantage of using diffracted light stems from the requirement that absorption must occur at distances very close to the electrode in order to attenuate light which is then diffracted. The comparatively long electrode provides high sensitivity, since the path length for absorption is determined by the electrode dimension, unlike methods based on transparent electrodes, where the effective path length is determined by the diffusion layer thickness. In addition, the diffracted light contains spatial information about the distribution of chromophores in the diffusion layer. In a fashion similar to X-ray diffraction experiments, it should be possible to extract diffusion profile shapes from optical diffraction patterns, with a resolution on the order of the wavelength of the light employed. The objective of the present effort is to develop the theory describing the response of light diffracted by an electrode to the generation of a chromophore at the electrode

(1) Winograd, N.; Kuwana, T. In "Electroanalytical Chemistry", Bard, A. J., Ed.; Marcel Dekker: New York, 1974; Volume 7.
(2) Kuwana, T. *Ber. Bunsenges. Phys. Chem.* **1973**, *77*, 858.
(3) Heineman, W. R. *Anal. Chem.* **1978**, *50*, 390A.
(4) Winograd, N.; Kuwana, T. *J. Electroanal. Chem.* **1979**, *23*, 333.
(5) Pruiksma, R; McCreery, R. L. *Anal. Chem.* **1979**, *51*, 2253.
(6) McCreery, R. L.; Pruiksma, R; Fagan, R. *Anal. Chem.* **1979**, *51*, 749.
(7) Skully, J. P.; McCreery, R. L.; *Anal. Chem.* **1980**, *52*, 1885.

0002-7863/81/1503-2524$01.25/0

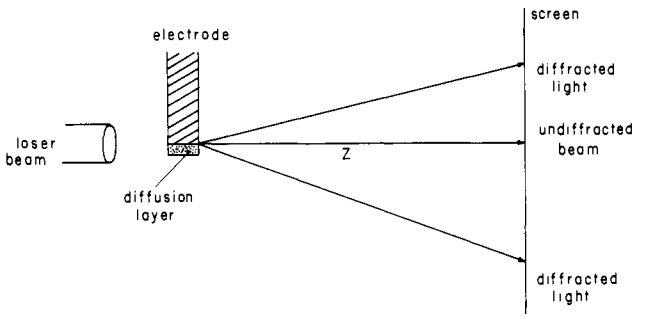

Figure 1. General experimental configuration for monitoring light diffracted by the electrode. Diffracted intensity is symmetrically distributed above and below the undiffracted beam.

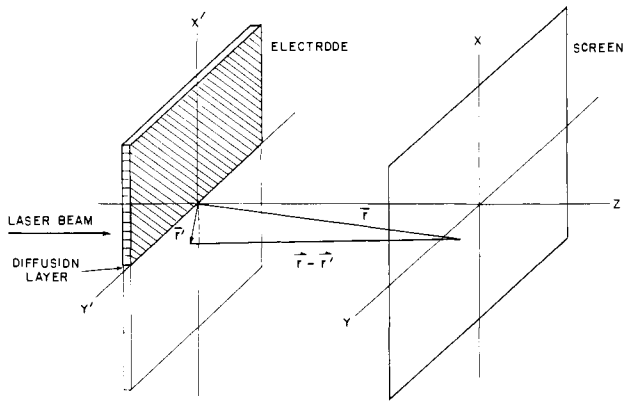

Figure 2. Coordinate system used in theoretical analysis. $|\vec{r} - \vec{r}'|$ is the propagation distance of light originating in the diffusion layer and arriving at some arbitrary point on the screen.

surface. Verification of theoretical predictions with the use of a test system is presented, and the advantages of spectroelectrochemistry with the use of diffracted light are discussed.

Theory

The objective of a theroetical analysis of the diffraction problem is to determine the dependence of the intensity of diffracted light appearing at a suitable target on the presence of electrogenerated chromophore. The intensity changes are most easily expressed as absorbance, which can be calculated from the ratio of intensity without chromophore to that with chromophore, at a particular target coordinate and time after initiation of electrolysis. As shown in Figure 1, the diffractive object is an edge with finite thickness along the optical axis. In theory, Maxwell's equations describe the diffraction of light by any object, but in practice the case of an edge with finite thickness along the propagation axis is extremely complex. As the z dimension of the edge shown in Figure 1 is made thin, however, the limit of an infinitely thin edge is approached, and this case has been examined in detail.[8] The only approximation necessary to predict diffraction by an electrode with or without electrogenerated chromophore is that the electrode diffracts light as if it were a thin edge. No other physical approximations are necessary in the theoretical analysis, and the validity of the thin edge assumption will be verified below.

Given the coordinate system shown in Figure 2, the diffracted intensity at a point (x,y,z) on the screen can be calculated from the Kirchoff–Huygens diffraction theory,[9] which essentially states that the amplitude of light at a point on the screen is a summation of all contributions from the original beam, as if each point in the beam at the electrode were a spherical radiator. Application of this principle at point $\vec{r} = (x,y,z)$ yields eq 1, describing the

$$A(\vec{r}) = \frac{ik}{2\pi}\int_{-\infty}^{\infty}\int_{-\infty}^{\infty}\frac{\exp(-ik|\vec{r} - \vec{r}'|)}{|\vec{r} - \vec{r}'|}\psi(x',y')\,dx'\,dy' \quad (1)$$

amplitude of the diffracted light at thescreen ($A(\vec{r})$). In this equation $\vec{r}' = (x',y',0)$ denotes the coordinates of a point on the plane of the side of the thin electrode nearest the screen ($z = 0$) and the wavenumber, k, is 2π divided by the wavelength of the incident light. The integration is over the plane of the trailing side of the electrode and $\psi(x',y')$ is the amplitude of the light on the plane. The amplitude function $\psi(x',y')$ has the following form. On the electrode itself $\psi(x',y')$ is zero, so, for the case pictured in Figure 2, $\psi(x',y') = 0$ for all $x' > 0$. On the remainder of the x',y' plane the amplitude is assumed to be determined by the absorptivity of the diffusion layer according to Beer's law. Thus $\psi(x',y')$ for $x' < 0$ is given by

$$\psi(x',y') = I_0^{1/2}(x',y')10^{-\epsilon bC(x')/2} \quad (2)$$

where $I_0(x',y')$ is the intensity of the incident light (a circular Gaussian beam in this case), ϵ is the extinction coefficient of the chromophore at the frequency of the incident light, b is the length of the electrode along the optical axis, and $C(x')$ is the concentration of the chromophore at the point x',y' and is independent of y' for the present case. $C(x')$ was calculated from standard linear diffusion equations, assuming the case of a stable electrogenerated chromophore. Note that the amplitude function ψ could represent any two-dimensional shape with arbitrary optical density. Thus slits, or holes, or any electrode configuration could be used, and the resulting diffraction calculated by using eq 1.

Equations 1 and 2 are a complete expression of the model for diffraction from a thin electrode. The electrode is assumed sufficiently thin (b sufficiently small) that eq 2 gives the amplitude of light at the trailing edge of the electrode and we therefore neglect surface effects and diffractive effects associated purely with the finite thickness of the electrode. With that assumption standard arguments of diffraction theory guarantee that eq 1 gives the amplitude reaching the screen and therefore yields the diffraction pattern. The mathematical approximations made below are only for convenience in evaluating the integral in eq 1 and, were they to fail, they could be discarded and the integral evaluated by direct numerical means.

Depending on the distance from the screen to the electrode, eq 1 can be treated by one of two standard simplifying approximations, the Fresnel and Fraunhofer approximations.[10] The Fresnel approximation is useful at relatively small distances and small diffraction angles. While it leads to an integral which can be evaluated by numerical methods, it does not give the most useful result. The Fraunhofer approximation, on the other hand, is useful at large distances from the electrode, and it yields a simpler expression for the diffracted amplitude. The Fraunhofer region is also more useful from an experimental standpoint because the diffracted light has been scattered significantly away from the main beam, whereas in the Fresnel region it would be necessary to monitor small changes in the main beam intensity. In the Fraunhofer region ($|\vec{r}| \gg |\vec{r}'|$) the distance $|\vec{r} - \vec{r}'|$ appearing in eq 1 is approximated by

$$|\vec{r} - \vec{r}'| \approx z + \frac{(x^2 + y^2)}{2z} - \frac{(xx' + yy')}{z} \quad (3)$$

in the exponential and simply by z, the distance from the electrode to the screen, in the denominator. The integral for $A(\vec{r})$ then becomes an ordinary Fourier transform.

$$A(\vec{r}) = \frac{ik}{2\pi z}\exp\left[-ik\left(z + \frac{(x^2 + y^2)}{2z}\right)\right] \times \int_{-\infty}^{\infty}\int_{-\infty}^{\infty}\exp\left[i\left(\frac{kx}{z}\right)x' + i\left(\frac{ky}{z}\right)y'\right]\psi(x',y')\,dx'\,dy' \quad (4)$$

(8) See for example: (a) Born, M.; Wolf, M. "Principles of Optics", Pergamon Press: New York, 1964; 3rd ed. (b) Herzberger, M. "Modern Geometrical Optics"; Interscience Publishers: New York, 1958. (c) Longhurst, R. S. "Geometrical and Physical Optics"; Longmans, Green and Co.: New York, 1957. (d) Marcuse, D. "Light Transmission Optics"; Van Nostrand Reinhold: New York, 1972.

(9) Kirchoff–Huygens diffraction theory is discussed in nearly every text on optics; for particularly clear treatments see ref 2d, p 31, and ref 8c, p 193.

(10) Reference 8c, p 195; ref 8d, p 39.

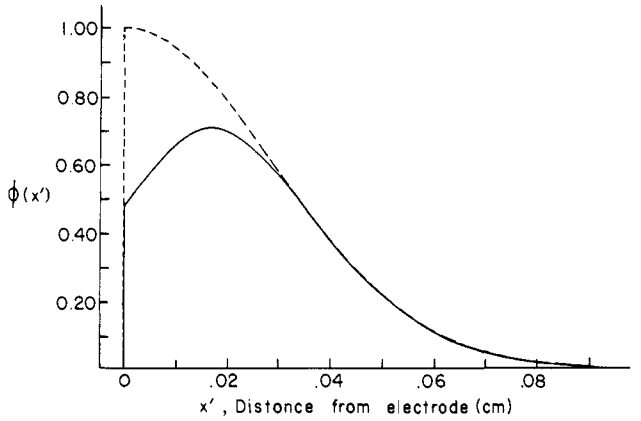

Figure 3. Amplitude function ($\phi(x')$) at the electrode. Dashed line represents a Gaussian laser beam truncated at its center by an opaque electrode. Solid line is same curve with an electrogenerated chromophore present.

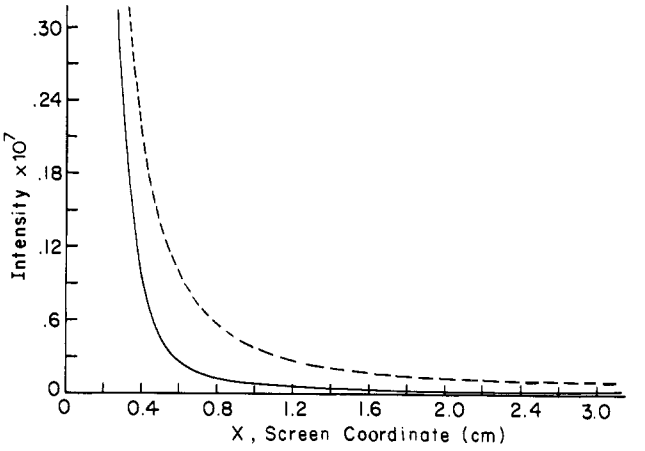

Figure 4. Diffraction patterns for amplitude distributions of Figure 3, calculated by Fourier transform and conversion from amplitude to intensity. Diffracted intensity is symmetric about $x = 0$. Dashed line is pattern for electrode without chromophore; solid line is pattern in the presence of chromophore.

This expression is valid for any arrangement of slits or apertures in the electrode, but it can be further simplified in the case shown in Figure 2 where only the diffraction pattern as a function of the screen coordinate x is desired. For this case with an incident circular Gaussian beam, $\psi(x',y')$ can be factored into a product of functions of x' and y'

$$\psi(x',y') = \phi(x')\rho(y') \tag{5}$$

and we can collect the result of the y' integration together with the other y dependent factors in eq 4 into a single function, $a(y)$, which is constant for the present experiment at a fixed value of y. The $A(\vec{r})$ is given by

$$A(\vec{r}) = \frac{ika(y)}{2\pi z} \exp[-ikz - ikx^2/2z] \int_{-\infty}^{\infty} \phi(x') \exp\left[i\left(\frac{kx}{z}\right)x'\right] dx' \tag{6}$$

with $\phi(x')$ given by

$$\phi(x') = i_0{}^{1/2}(x')10^{-\epsilon bC(x')/2} \tag{7}$$

where $i_0(x')$ is the intensity of the incident beam as a function of x' and ϕ is the x' dependent factor when $I_0(x',y')$ in eq 2 is factored into a product of functions of x' and y'. Figure 3 shows the function $\phi(x')$ for an electrode edge with and without chromophore present. The dashed line is the amplitude of a Gaussian laser beam partially occluded by the electrode, and the solid line shows the same profile after generation of chromophore, assuming linear diffusion.

When $A(\vec{r})$ from eq 6 is converted to intensity ($|A(\vec{r})|^2$), the term preceding the integral becomes a constant independent of the presence of chromophore or the x coordinate on the screen. Thus it is only necessary to consider the integral of eq 6, which is simply the Fourier transform of the amplitude function $\phi(x')$. Once $\phi(x')$ is calculated from the properties of the chromophore, the integral can be evaluated by a number of standard numerical techniques including the fast Fourier transform algorithms often used in X-ray crystallography. Thus if the concentration function, $C(x')$, and the intensity profile of the incident laser beam are known, the intensity $|A(\vec{r})|^2$ can be calculated as a function of the screen coordinate x for fixed values of z and y. Furthermore, if only relative intensities are desired as a function of screen coordinate, the pre-exponential constant in eq 6 need not be calculated. It is worth noting that it is generally true that the Fraunhofer diffraction pattern is the Fourier transform of the amplitude function which generated it.[11] For example, a single slit produces a pattern with a large central maximum and secondary maxima which diminish in intensity with distance from the central maximum. Each maximum is a Fourier component, with the contribution diminishing with higher spatial frequency (larger angles). When the sinusoidal components represented by these maxima are summed, one obtains the original square wave shaped profile of the slit. For the present experiment, a single edge was used because of ease of construction and alignment. The results of calculations based on the Fourier approach for an edge electrode are discussed below.

Equation 6 also provides the theroetical basis for the inversion process of determing the shape of any concentration profile from the Fraunhofer diffraction pattern. The process is analogous to determining structures from X-ray diffraction, except optical wavelengths are used to determine profiles with features with dimensions on the order of the wavelength employed. Applying an inverse Fourier transform to both sides of eq 6 results in eq 8. Thus if the amplitude at the screen ($A(\vec{r})$) is known, $\phi(x')$

$$\phi(x') = \frac{1}{ia(y)} \exp[ikz + ikx^2/2z] \int_{-\infty}^{\infty} \exp\left[-i\frac{kx'}{z}x\right] A(\vec{r})\, dx \tag{8}$$

can be determined and the concentration vs. x' profile deduced. Work on the inversion problem is in progress, but the present paper is directed toward assessing the validity of the theory outlined above.

To predict a diffraction pattern for an absorbing diffusion profile intercepting a Gaussian beam (Figure 3, solid curve) the Fourier transform of the amplitude vs. x profile, $\phi(x')$, was evaluated. Figure 4, dashed curve, shows the squared modulus of the Fourier transform of Figure 3 (dashed curve), representing a bare edge without chromophore. While only positive values of the screen coordinate x are shown, the pattern is symmetric about $x = 0$. Note also that intensity rather than amplitude is plotted to permit experimental comparison. The diffraction pattern for an edge shown in Figure 4 does not display the classical oscillatory Fresnel pattern but instead shows smooth behavior analogous to the $1/x^2$ intensity pattern expected in the Fraunhofer region for an illuminated bare edge. Thus the dashed curve in Figure 4 shows the diffraction from a partially obstructed Gaussian beam viewed at great distance, rather than a completely illuminated edge viewed in the Fresnel region, close to the edge. In Figure 4, the solid curve shows a transform of the same electrode with an electrogenerated absorber included. The parameters which served as input to the Fourier transform computer algorithm correspond to the experimental quantities used for verification. By comparison of the two curves in Figure 4, it is apparent that the larger angles are attenuated more, a point which is more obvious in Figure 5, which shows absorbance calculated from the curves in Figure 4. The larger angles represent the higher Fourier frequencies required to synthesize the original amplitude distribution at the electrode. Thus it is reasonable that the higher angles are attenuated more,

(11) Gaskill, J. P. "Linear Systems, Fourier Transforms and Optics"; John Wiley & Sons: New York, 1978; p 376.

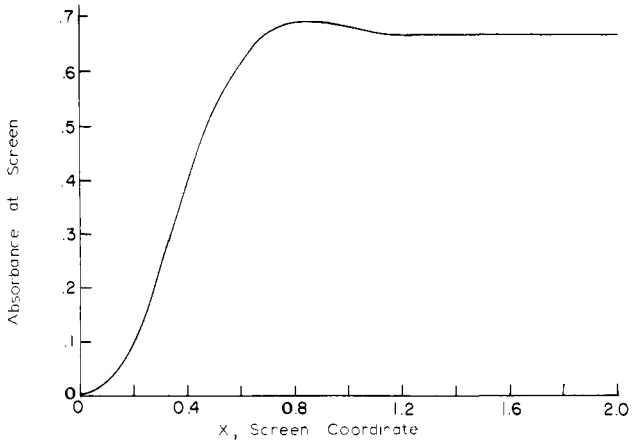

Figure 5. Absorbance measured at the screen, as a function of screen coordinate. Absorbance was calculated from Figure 4 and is defined as the base 10 logorithm of the ratio of diffracted intensity with chromophore absent to that with chromophore present.

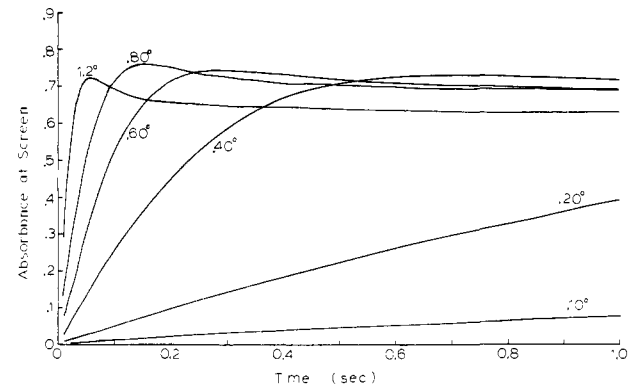

Figure 6. Theoretical absorbance vs. time profiles at particular diffraction angles. Reference intensity for absorbance calculation was that occurring before electrogeneration of chromophore began. Electrode path length = 0.5 mm, ϵ for chromophore = 10750, diffusion coefficient = 1.49×10^{-5}, bulk precursor concentration = 1.2×10^{-3} M.

since they describe the sharpness of the edge. As the chromophore is generated, the edge becomes less sharp, and the higher Fourier frequencies are less important. Viewed slightly differently, the optical density distribution near the electrode in the absence of chromophore is composed of higher Fourier frequencies than the more rounded distribution when chromophore is present.

As time progresses from the start of electrolysis, the shape of the profile depicted in Figure 3 changes as chromophore diffuses away from the electrode. By evaluating the Fourier transform in eq 6 for a series of amplitudes, $\phi(x')$ corresponding to concentration profiles at different times, a plot of diffracted intensity at a particular angle can be obtained as a function of time after beginning the electrolysis. Figure 6 is such a plot, for uncomplicated linear diffusion, where the absorbance being plotted is the log of the ratio of intensity before to that after electrolysis began. Several important features which indicate the value of the technique can be observed in this plot. First, the response is very fast, particularly at high angles, with 0.55 absorbance units being reached in 25 ms at 1.2°. This absorbance is 76 times that expected for an optically transparent electrode experiment of conventional design. Second, the absorbance at long times reaches a constant value (0.65) regardless of angle. The value calculated from Beer's law by using the electrode dimension along the optical axis as a path length and a chromophore concentration equal to the bulk precursor concentration is 0.65. This limiting value corresponds to the situation where chromophore has filled the region near the electrode, up to the original bulk concentration of precursor. This is optically equivalent to attenuating the entire input beam, so all diffracted light is attenuated equally at long times. Note that the higher angles reach this limiting value faster,

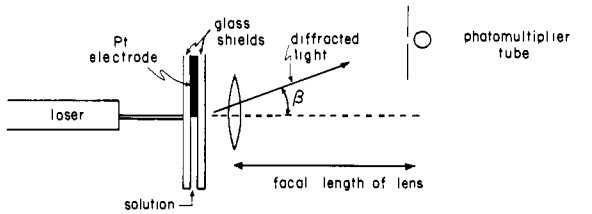

Figure 7. Configuration for diffraction experiment. Reference and auxiliary electrodes were in solution below the working electrode compartment and solution was held near the working electrtode by capillary action. The focal length of the lens was 36.5 cm. The aperture preceding the photomultiplier was a 0.8 mm diameter hole.

again implying that higher angles correspond to higher spatial frequencies, which are derived from regions close to the electrode. There is not a one-to-one correspondence between diffraction angle and distance from the electrode, but it is true that higher angles have a greater contribution from events close to the electrode surface. For light diffracted at 1.2°, the absorbance reaches the limiting value in roughly 100 ms, corresponding to a diffusion layer thickness of 11 μm (17 wavelengths of 632.8-nm light). So diffraction at 1.2° has its greatest contributions from events within about 20 wavelengths of the electrode surface.

The third conclusion derived from theory is that the diffracted light contains spatial information, since the absorbance vs. time curve is highly dependent on angle. As the shape of the diffusion layer changes, so does the distribution of diffracted light. It should be possible to invert the diffraction pattern to obtain the distribution of chromophore as a function of distance from the electrode. Despite the fundamental nature of concentration vs. distance profiles to questions about mass transport and reaction mechanisms, they have not been observed experimentally with an accuracy better than about 20%. A final consideration of the diffractive approach is its potentially high sensitivity. The path length is not dictated by the diffusion layer thickness but rather by the electrode length. While the theory assumes a thin electrode edge, it is nevertheless possible that a long (~1 cm) electrode could be used to examine weak chromophores.

Experimental Section

The optical arrangement is shown in Figure 7. Solution entered the electrode region from below, from a cell containing the reference and auxiliary electrodes. The potential was controlled with a commercial potentiostat triggered by a laboratory computer which also monitored the signal from the detector. The platinum electrode was 0.5 mm along the optical axis, and the exposed edge was polished to a mirror finish with alumina. The glass shields on the electrode assured linear diffusion and defined the boundaries of the cell. The beam from a 5 mW He–Ne laser (632.8 nm) was directed onto the electrode by a beam steering device, and the electrode could be rotated relative to the beam. The electrode was first positioned so that part of the beam was reflected off the active surface, then the electrode was rotated so the reflected and nonreflected beams coincided. This process assured that the active electrode face was parallel to the input beam. The detector was a 1P28 photomultiplier operated with conventional electronics and interfaced to the computer. Given that the diffracted intensity is symmetric about the origin of the screen coordinate, the detector was placed in the shadow region of the electrode to minimize stray light from reflection or other nondiffractive scattering. The detector was positioned with micrometer stages, and the entire apparatus was mounted on a vibration isolated optical table.

The lens following the cell served to impose the Fraunhofer condition necessary to validate the Fourier transform. A dectector positioned on the focal plane of the lens will be sampling light which was parallel when entering the lens. The requirement for parallel input light to the lens automatically validates the Fraunhofer approximation, since the screen position is effectively at infinity. Each point on the focal plane of the lens represents a particular Fourier frequency, dictated by the following expression:

$$X = Zm\lambda/2L \tag{9}$$

where Z = the focal length of the lens, m = the component of the numerical Fourier transform, and L = the physical width of the input to the transform algorithm.

The theory discussed above assumed the entire diffraction process occurred in a medium of constant refractive index, but in the experiment

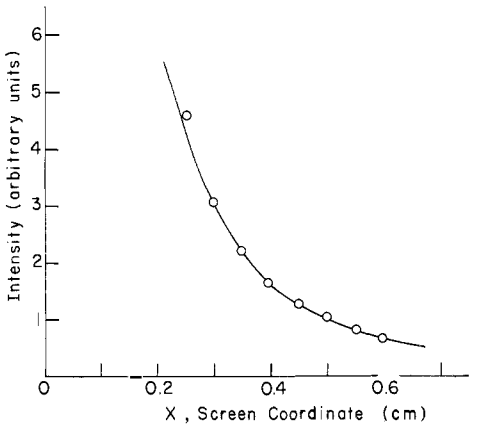

Figure 8. Comparison of theory and observation for diffraction of a Gaussian laser beam by a 0.5 mm thick electrode edge. Solid line is theoretical intensity and points are observed. The y axis scale was adjusted for best fit, so the shapes of the curves are meaningful, but absolute intensity comparisons are not.

a phase boundary between acetonitrile (n = 1.34) and air (n = 1.00) occurs. A correction for this phase boundary is not necessary because the change in direction at the interface is compensated by the diffraction process. Suppose for the moment that the entire experiment were performed in a solvent of refractive index x_s, where the wavelength is shorter than in air ($\lambda_s = \lambda_{air}/n_s$). Equation 9 would become:

$$\sin \alpha = \frac{X_s}{Z_s} = \frac{m\lambda_a}{Zn_sL} \tag{10}$$

where α is the scattering angle within the solvent. When this scattered light passes into air, the observed angle (β in Figure 7) will be larger than α according Snell's law:

$$\sin \alpha = (\sin \beta)/n_s \tag{11}$$

Substituting into eq 10,

$$\sin \beta = \frac{X_a}{Z_a} = \frac{m\lambda_a}{2L} \tag{12}$$

Notice that eq 12 is identical to eq 9, except β is the apparent diffraction angle measured in air.

The test system employed was the one-electron oxidation of trianisylamine (TAA) to its cation radical at 0.6 V vs. SCE in acetonitrile.[12] The diffusion coefficient[12] in 0.1 M TEAP is 1.49×10^{-5} cm^2/s and the molar absorptivity[13] at 632.8 nm is 10750 M^{-1} cm^{-1}. TAA was obtained as a gift from R. N. Adams (University of Kansas). Tetraethylammonium Perchlorate (TEAP) was obtained from Eastman and used without further purification.

Results

A comparison of theoretical and experimental diffraction patterns for a bare electrode without chromophore is shown in Figure 8. The measured intensity was uncalibrated, so its magnitude was scaled until the best fit with theory was obtained. The distance scale is absolute, so Figure 8 indicates that the diffracted light changes with angle as predicted from theory. These results also indicate that a 0.5 mm thick edge diffracts light in the same fashion as expected from an infinitely thin edge.

Rather than constructing diffraction patterns in the presence of chromophore at a particular time after electrolysis began, it is simpler and more informative to observe intensity changes at a particular screen coordinate as a function of time. Figure 9 shows absorbance vs. time plots monitored at the focal plane at various angles relative to the optical axis. The reference intensity for the absorbance calculation was the intensity before the potential step occurred. At times longer than the 1 s shown here, all curves at all angles studied (up to 1.2°) reached a value of 0.65 absorbance units. The theoretical absorbance vs. time curves shown in Figure 6 were calculated for the experimental conditions producing Figure 9.

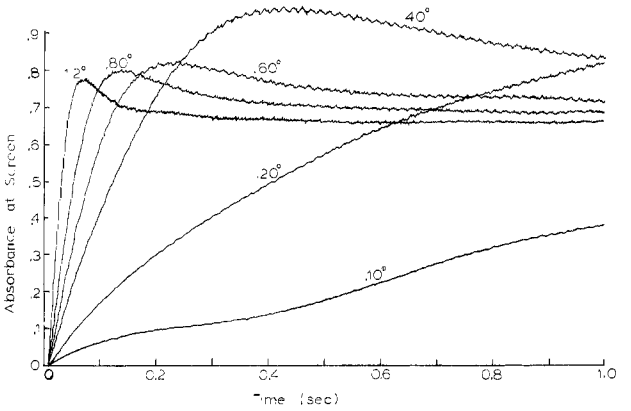

Figure 9. Experimental absorbance vs. time curves as a function of diffraction angle for the oxidation of TAA (1.2 mM) in acetonitrile. Reference intensity for absorbance calculations is the intensity preceding electrolysis. Electrode length along optical axis = 0.5 mm.

Discussion

The agreement between theory and experiment shown in Figures 6 and 9 is quite good, indicating that the Fourier transform approach (the Fraunhofer approximation) adequately describes the effect of an electrogenerated chromophore on diffraction from an edge. The approximation of a 0.5-mm electrode by a thin edge appears to introduce little error, at least under the conditions used here. Furthermore, preliminary experiments with a 1.3-cm electrode show good agreement with theory, even at short electrolysis times (~25 ms) where the diffusion layer is very thin relative to the electrode dimension along the optical axis. Thus the Fraunhofer region appears insensitive to the electrode thickness within the limits examined here. One would predict that the 1.3-cm edge would degrade the spatial information in the diffracted light, leading to a trade-off between spatial resolution and sensitivity. Nevertheless, the long-path electrodes will be useful for quantitative analysis, particularly at long (>1 s) times, where the absorbance has reached the Beer's law value. A different potential source of error is the phase shift caused by small changes in refractive index when the substrate is oxidized. This error also appears small, a reasonable observation when one considers that methods used to measure refractive index changes in the diffusion layer require concentrations about 100 times larger than those used here. The most noticeable deviations between theory and experiment occur at small angles (0.4° or less) where the accuracy of measuring the angle is poorest. In addition, small errors in alignment and positioning of the electrode relative to the beam affect the results at small angles more than at large angles. Variations in small-angle response with positioning are evident experimentally and will be decreased with more accurate alignment.

The experimental results verify that the major theoretical predictions are valid. First, the response is fast at large (1.2°) angles, with 0.8 absorbance units being attained in 70 ms. Higher angles and faster response are possible, but the present laser lacked sufficient power. The experimental value at 70 ms and 1.2° is 120 times that obtained for an optically transparent electrode under similar conditions. Second, the observed absorbance reaches a constant value at long times, independent of angle. As predicted by theory, this value is the Beer's law result corresponding to a nearly homogeneous distribution of chromophore in the region near the electrode. Third, the variation in diffracted intensity with angle and time indicates the pattern is sensitive to spatial distribution of chromophore, since each distinct pattern is derived from a different intensity distribution at the electrode. A Fourier inversion of the diffraction pattern will then yield the chromophore distribution as a function of time. Accurate experimental diffusion profiles can be used for examining both simple and complex

(12) Winograd, N.; Kuwana, T. *Anal. Chem.* **1971**, *43*, 252.
(13) Pruiksma, R, Ph.D. Thesis, Ohio State University, 1980.

processes associated with charge transfer when the dominant mode of mass transport is diffusion. In addition, concentration profiles for electromigration or turbulent conditions could be obtained, elucidating a variety of mass transport processes. Different electrode shapes, including microelectrodes, which have quite different diffusion profiles, are amenable to the same approach. Finally, the results demonstrate that absorbance is proportional to path length, so an electrode with a longer dimension along the optical axis will have higher sensitivity to the presence of chromophores. Unlike most spectroelectrochemical measurements, where effective path length is dictated by the diffusion process, the diffractive approach allows sampling of distances close to the electrode so long paths can be employed.

Given the theoretical basis of diffractive spectroelectrochemistry, future efforts will be directed toward establishing the practical limits on electrode length, time resolution, and sensitivity. In addition, the inversion process producing a diffusion profile shape from a diffraction pattern will be examined. The improved speed, sensitivity, and information content of the diffractive approach should significantly increase the generality of spectroelectrochemical techniques.

Acknowledgment. This work was supported by grants from NSF (CHE-7828068) and NIMH (24812).

Two-Dimensional Rotational Spin-Echo Nuclear Magnetic Resonance in Solids: Correlation of Chemical Shift and Dipolar Interactions

M. G. Munowitz,[1a] R. G. Griffin,*[1b] G. Bodenhausen,[1b,c] and T. H. Huang[1b]

Contribution from the Francis Bitter National Magnet Laboratory, Massachusetts Institute of Technology, Cambridge, Massachusetts 02139, and Department of Chemistry, Harvard University, Cambridge, Massachusetts 02138. *Received August 11, 1980*

Abstract: Two-dimensional NMR techniques which separate the chemical shift and heteronuclear dipolar interactions are applied to samples spinning at the magic angle. Because of the inhomogeneous nature of the two interactions, rotational echoes are observed in the time domain of each dimension. The corresponding Fourier transforms yield rotational sideband spectra which provide information on the principal values and relative orientations of the shift and dipolar tensors, and, from the latter, internuclear distances may be calculated. The techniques therefore provide a means for obtaining structural data, for example, $^{13}C-^{1}H$ and $^{15}N-^{1}H$ distances, in powder samples.

I. Introduction

One of the principal aims of high-resolution, solid-state NMR techniques is the suppression of homo- and heteronuclear dipolar interactions and the recovery of underlying chemical shifts and scalar spin couplings. Nevertheless, the development of high-resolution methods has suggested ways whereby dipolar couplings may be retained, and since these interactions contain information on internuclear distances and directions, they are clearly of considerable chemical significance. A particularly simple example is the observation of dipolar splittings between magnetically dilute spin pairs such as $^{13}C-^{14}N$ or $^{13}C-^{13}C$.[2-5] In these cases, the proton-decoupled ^{13}C spectra show dipolar splittings from adjacent ^{14}N or ^{13}C nuclei. In addition, it has been demonstrated that a number of other chemically interesting groups constitute magnetically dilute systems, two examples being $^{13}C-^{1}H$ and $^{14}N-^{1}H$. In the case of ^{14}N, which possesses a quadrupole moment, the lines are dispersed over 10^5-10^6 Hz, and the $^{14}N-^{1}H$ couplings, which are of the order of 10–15 kHz, are easily seen in single crystal spectra as small splittings on well-separated resonances.[6] However, the situation where one interaction dominates the other is not commonly encountered. More often, for example, in $^{13}C-^{1}H$ spectra, the dispersion of shifts is approximately the same size as the heteronuclear dipolar interaction, and consequently there is considerable overlap in the spectra, particularly in polycrystalline samples.

The *separation* of chemical shift and heteronuclear dipolar interactions in the NMR spectra of single crystals has recently been the subject of a number of two-dimensional experiments.[7,8] These methods, which are applicable to other inhomogeneous interactions,[9] generally allow for the evolution of the dipolar Hamiltonian during an interval prior to a proton-decoupled sampling period. Chemical shift spectra obtained in this manner receive information from the dipolar Hamiltonian in the form of a modulation, and a second Fourier transformation[10] separates the two interactions. This experiment is also applicable to powder samples[11,12] but when overlap from magnetically inequivalent nuclei occurs, the spectra are difficult to interpret.

The separation of overlapping chemical shift powder spectra can be accomplished with magic angle sample spinning (MASS).[13,14] When the spinning speed greatly exceeds the

(1) (a) Harvard University; (b) Francis Bitter National Magnet Laboratory; (c) Laboratory for Physical Chemistry, ETH—Zentrum, CH-8092 Zurich, Switzerland.
(2) (a) R. G. Griffin, A. Pines, and J. S. Waugh, *J. Chem. Phys.*, **63**, 3676 (1975); (b) M. E. Stoll, R. W. Vaughan, R. B. Saillant, and T. Cole, *ibid.*, **61**, 2896 (1974).
(3) S. Kaplan, A. Pines, R. G. Griffin, and J. S. Waugh, *Chem. Phys. Lett.* **25**, 78 (1974).
(4) H. van Willigen, R. G. Griffin, and R. A. Haberkorn, *J. Chem. Phys.*, **67**, 5855 (1977).
(5) D. L. van der Hart, *J. Magn Reson.*, **24**, 467 (1976).
(6) R. E. Stark, R. A. Haberkorn, and R. G. Griffin, *J. Chem. Phys.*, **68**, 1996 (1978).
(7) R. K. Hester, J. L. Ackerman, B. L. Neff, and J. S. Waugh, *Phys. Rev. Lett.* **36**, 1081 (1976).
(8) E. F. Rybaczewski, B. L. Neff, J. S. Waugh, and J. S. Sherfinski, *J. Chem. Phys.*, **67**, 1231 (1977).
(9) G. Bodenhausen, R. E. Stark, D. J. Ruben, and R. G. Griffin, *Chem. Phys. Lett.* **67**, 424 (1979).
(10) W. P. Aue, E. Bartholdi, and R. R. Ernst, *J. Chem. Phys.*, **64**, 2229 (1976).
(11) M. E. Stoll, A. J. Vega, and R. W. Vaughan, *J. Chem. Phys.*, **65**, 4093 (1976).
(12) M. Linder, A. Hohener, and R. R. Ernst, *J. Chem. Phys.*, **73**, 4959 (1980).

0002-7863/81/1503-2529$01.25/0